Front. Phys. 11(5), 117404 (2016)
DOI 10.1007/s11467-016-0572-7

RESEARCH ARTICLE

Robustness of *s*-wave pairing symmetry in iron-based superconductors and its implications for fundamentals of magnetically driven high-temperature superconductivity

Jiangping Hu[1,2,3,†], **Jing Yuan**[1]

[1] *Institute of Physics, Chinese Academy of Sciences, Beijing 100190, China*
[2] *Department of Physics, Purdue University, West Lafayette, IN 47907, USA*
[3] *Collaborative Innovation Center of Quantum Matter, Beijing 100871, China*
Corresponding author. E-mail: †*jphu@iphy.ac.cn*

Received November 9, 2015; accepted March 2, 2016

Based on the assumption that the superconducting state belongs to a single irreducible representation of lattice symmetry, we propose that the pairing symmetry in all measured iron-based superconductors is generally consistent with the A_{1g} *s*-wave. Robust *s*-wave pairing throughout the different families of iron-based superconductors at different doping regions signals two fundamental principles behind high-T_c superconducting mechanisms: (i) the correspondence principle: the short-range magnetic-exchange interactions and the Fermi surfaces act collaboratively to achieve high-T_c superconductivity and determine pairing symmetries; (ii) the magnetic-selection pairing rule: superconductivity is only induced by the magnetic-exchange couplings from the super-exchange mechanism through cation-anion-cation chemical bonding. These principles explain why unconventional high-T_c superconductivity appears to be such a rare but robust phenomena, with its strict requirements regarding the electronic environment. The results will help us to identify new electronic structures that can support high-T_c superconductivity.

Keywords iron-based superconductors, cuprates, unconventional superconductivity, high-temperature superconductors

PACS numbers 74.20.Mn, 74.25.-q, 74.20.-z, 74.70.Xa

1 Introduction

The discovery of iron-based superconductors [1] eight years ago removed the perception that cuprates were the primary determining factors of high-T_c superconductors in correlated electron systems, and it generated much hope for a solution to the decades-old problem of the non-BCS (Bardeen, Cooper and Schrieffer) high-T_c mechanism. There were fundamental reasons for such optimism. Iron-based superconductors were quickly shown [2–4] to share many common electronic properties with cuprates, including a close proximity to an antiferromagnetic (AFM) order phase [5]. The similarity between the two superconductors strongly suggests that there should be one unified high-T_c superconductivity mechanism. In the meantime, iron-based superconductors exhibit many distinct physical properties when compared to cuprates. The differences between these two materials also enable us to determine the side effects that are irrelevant to the superconducting mechanism.

However, over the past few years, the optimism has diminished with the discovery of more iron-based superconductors [3, 4] and a comprehensive understanding of all of the materials became increasingly difficult. In particular, pairing symmetries in iron-based superconductors have recently become more controversial [6]. A variety of new possible pairing symmetries were proposed, and many theories suggested that there is no universal pairing symmetry between iron-based superconductors [6–8]. Pairing symmetries are material and doping dependent, and this situation is similar to the research status of cuprates in the early 1990's before the *d*-wave pairing symmetry was finalized [9]. The *d*-wave pairing symmetry in cuprates is widely acknowledged as the major evidence that differentiates cuprates from conventional BCS-type *s*-wave superconductors. The robustness of the *d*-wave pairing in cuprates is one of the main supports

for magnetically driven high-T_c superconducting mechanisms [10, 11]. Thus, without a consensus on the pairing symmetry in iron-based superconductors, it is difficult to understand how the study of iron-based superconductors can help to advance the understanding of high-T_c superconducting mechanisms.

The pairing symmetry controversy in iron-based superconductors was largely caused by "top-to-bottom" theoretical studies. The study of correlated electron materials or materials that are believed to be in that category has been customized to standardized models and methods [10, 11], which are inherited from previous extensive research of cuprates. After the discovery of iron-based superconductors, extended versions of these standardized models, such as Hubbard-type [6] or "t-J"-type models [12–14], were immediately deployed. The pairing symmetries in iron-based superconductors were analyzed using a variety of methods under both strong and weak interaction regions [6]. In cuprates, the d-wave pairing symmetry is consistently obtained by all these methods. However, the theoretical predictions of the pairing symmetries in iron-based superconductors are in turmoil [6]. In particular, as Fermi surfaces in iron-based superconductors can vary significantly in different doping regions, as well as in different families of iron-based superconductors, standard theoretical methods, which result from their high sensitivity to changes in the Fermi surfaces, suggest that the pairing symmetries would also vary significantly.

However, if we take the "bottom-up" approach and examine the experimental evidence for the pairing symmetries in iron-based superconductors, we note that all experimental investigations that directly probe the superconducting pairing symmetry point to a universal s-wave pairing symmetry in all measured materials [15], including the recently discovered materials [16–18]. Thus, the robust s-wave pairing symmetry in iron-based superconductors is not only a challenge, but also offers an opportunity to establish fundamentals in magnetically driven high-T_c superconducting mechanisms.

2 Pairing symmetries and gap functions

Before discussing the experimental evidence, for clarity, a few acceptable assumptions and notations should be noted. First, we focus on the uniform superconducting state. In other words, the state has the original lattice translational symmetry. Second, we assume that the pairing in iron-based superconductors is a spin-singlet. This assumption has been supported by many experiments throughout different families of iron-based superconductors [3, 4, 6]. Third, in this study, unless otherwise stated, we used the 1–Fe unit cell to label the momentum space [19]. In this case, because the natural unit cell for iron-based superconductors is a 2–Fe unit cell, in the 11 (FeSe), 111 (NaFeAs), or 1111 (LaOFeAs) types of materials that have a non-symmorphic space group $P4/nmm$, and the 122 ($BaFe_2As_2$) type of materials that has space group $I4/mmm$, the $\boldsymbol{Q}_1 = (\pi, \pi, 0)$ and $\boldsymbol{Q}_2 = (\pi, \pi, \pi)$ in the reciprocal lattice of the 1–Fe unit cell are reciprocal lattice vectors in the original 2–Fe unit cell [7]. In the following section of the paper, as we primarily focus on the two-dimensional (2D) electronic structures of the building block, the FeAs/Se layer, which is equivalent to setting $k_z = 0$ for the bulk materials, both $\boldsymbol{Q}_1$ and $\boldsymbol{Q}_2$ are reduced to $\boldsymbol{Q} = (\pi, \pi)$. Finally, as mentioned in Ref. [7], there are two types of pairing that do not break translational symmetries with respect to the 2–Fe unit cell in iron-based superconductors. These are the normal pairing, which is between two particles with opposite momentum, namely, $(\boldsymbol{k}, -\boldsymbol{k})$, and the η pairing, which is specified by corresponding paired momentum, as $(\boldsymbol{k}, -\boldsymbol{k} + \boldsymbol{Q})$. The difference between these two types of pairings is classified by the parity difference with respect to the center on the nearest-neighbor (NN) Fe–Fe bonds. Because of this difference, the mixture of normal and η pairing is also not a pure state. Because it is almost impossible to obtain pure η pairing under reasonable conditions, we will also ignore the η pairing below.

Assuming that the superconducting state is a pure state, the pairing symmetry is shown in superconducting gap functions in the reciprocal space. For iron-based superconductors, if we take $k_z = 0$ and ignore spin-orbital couplings, which are known to be small [20], the normal pairing can be classified by the D_{4h} group, which is the same as cuprates. With the exception of the A_{1g} s-wave, all other pairing symmetries have fixed gapless nodes along some high symmetry lines in the reciprocal space. In Fig. 1, we draw four typical Fermi surface topologies. Figure 1(a) represents heavily hole-doped iron-pnictides such as KFe_2As_2. There are three hole pockets at the zone center (Γ) and four small hole pockets at the zone corner (M). With increasing electron doping, the four hole pockets at the zone corner become two electron pockets, as shown in Fig. 1(b), which represents the typical Fermi surfaces in iron-pnictides within large doping regions. It is also important to note that depending on the doping and materials, the number of hole pockets at the zone center, as shown in Figs. 1(a) and (b), can also vary. For example, in the bulk $FeSe_xTe_{1-x}$ materials [15], there are only two hole pockets at the zone center and in the heavily electron-doped LiFeAs [15], there may be just one hole pocket at the

zone center. With increased electron doping, the hole pockets at the zone center can be suppressed completely, as shown in Fig. 1(c). The heavily electron-doped iron-pnictides and many iron-chalcogenides, including the superconducting KFe_2Se_2 [21], the superconducting single layer FeSe grown on the $SrTiO_3$ substrate [22–24], and (Li,Fe)OHFeSe [16–18], have such a typical Fermi surface topology. Away from the $k_z = 0$ plane, heavily electron-doped KFe_2Se_2 can also have a small three-dimensional (3D) electron pocket, as shown in Fig. 1(d), where a small electron pocket appears at the zone center at $k_z = \pi$ [25].

In the presence of the hole pockets at the zone center, as shown in Figs. 1(a) and (b), a direct measurement of the gap functions on the hole pockets can determine the pairing symmetry. The angle resolved photoemission spectroscopy (ARPES) has been employed to measure a variety of iron-based superconductors [15, 26] that exhibit hole pockets at the zone center, including hole doped $Ba_{2-x}K_xFe_2As_2$, electron doped $Li(Na)Fe_{1-x}Co_xAs$, isovalent doped $BaFe_2(As_{1-x}P_x)_2$ and $BaFe_{2-x}Ru_xAs_2$, and $FeSe_{1-x}Te_x$. There are two common results regarding the measured gap functions of the hole pockets. *First, the inner smallest hole pocket always has the largest full superconducting gap that is almost isotropic. Second, the superconducting gap sizes on the hole pockets generally follow the rule: larger gaps on smaller hole pockets [15].* These two facts are valid in all measured doping regions. If the superconducting state is a pure state, the two common results are only consistent with the s-wave pairing. In fact, even if we do not assume a pure state, these results suggest that the s-wave pairing must be the dominant component.

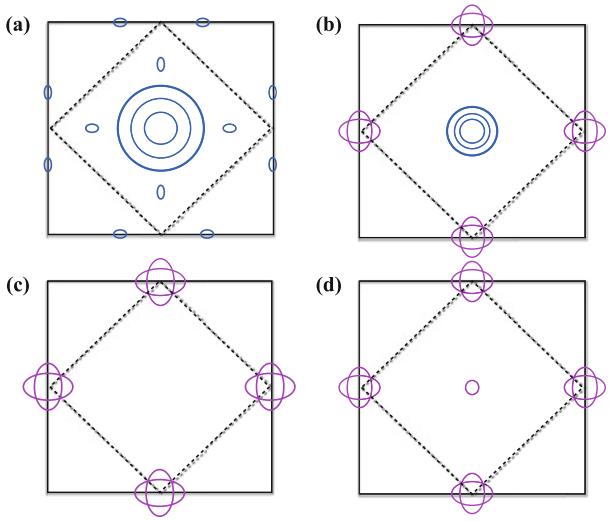

Fig. 1 The typical Fermi surface topologies of iron-based superconductors: **(a)** Heavily hole doped (KFe_2As_2); **(b)** Near optimally doped iron-pnictides; **(c)** Heavily electron doped (single layer FeSe/STO, (Li,Fe)OHFeSe and KFe_2Se_2 at $k_z = 0$); **(d)** KFe_2Se_2 at $k_z = \pi$.

In the case shown in Figs. 1(c) and (d), in which there is no hole pockets at the zone center, a full gap structure on the electron pockets [16–18, 21] was also universally observed. This full gap structure is generally only consistent with the s-wave pairing symmetry. For a bulk material, the nodes on electron pockets are inevitable if it is a d-wave pairing state [27]. In the case of Fig. 1(d), which represents the Fermi surfaces of KFe_2Se_2 at $k_z = \pi$, there is another direct evidence for the s-wave pairing symmetry: the small electron pocket at the zone center has almost isotropic full gap [21, 25]. A case that needs to be specifically addressed is the single layer FeSe/STO [22–24]. In this case, a full gap structure on electron pockets, in principle, can be consistent with the B_{1g} d-wave. However, if we consider the hybridization between two electron pockets at the zone corner caused by the spin–orbital couplings and the lattice symmetry breaking induced by the substrate, gapless nodes must generally appear in the B_{1g} d-wave state. Therefore, a full gap structure on electron pockets is also only consistent with an s-wave state.

In addition to the direct gap function measurements of ARPES, scanning tunneling microscopy (STM) also reveals a full gap structure in many different materials [3]. The measurements for on tunneling junctions also support the s-wave pairing symmetry [2].

It is also important to note that there is indirect evidence to support the d-wave pairing in some materials of iron-based superconductors. For example, possible d-wave pairing symmetry is indirectly indicated in KFe_2As_2 by thermal conductivity measurements and pressure effect [28]. However, this indirect indication is not conclusive. The thermal transport probes the existence of low-energy excitations, namely the existence of superconducting nodes on Fermi surfaces. However, it does not specify the structure of the nodes. In fact, the ARPES measurements in KFe_2As_2 have shown that there are possible gapless nodes in the outer hole pockets [29, 30] but the inner hole pocket from the $d_{xz/yz}$ orbitals is fully gapped. Nodes have also been directly observed by ARPES in $BaFe_2(As_{1-x}P_x)_2$ on the hole pocket that has the largest k_z dispersion at the zone center [31]. These nodes are not located on the high symmetry lines. Thus, they are not protected by symmetry. The development of the accidental nodes may be related to the large c-axis dispersion on the hole pocket of the $d_{xz/yz}$ orbitals in both KFe_2As_2 and $BaFe_2(As_{1-x}P_x)_2$ [32].

In summary, the full gap structure on Fermi pockets observed in a variety of iron-based superconductors at

different doping regions is only consistent with the A_{1g} s-wave pairing symmetry. The appearance of the largest isotropic gap on the smallest hole pocket suggests that the s-wave component dominates even if the superconducting state is not a pure state.

3 Theoretical results on pairing symmetries of iron-based superconductors

By performing extensive research on cuprates, we have been accustomed to the use of two types of standard models to investigate correlated electron systems. The first type of standard models includes the band structure near the Fermi surfaces and the effective local repulsive interactions in the spirit of the Hubbard model. The second type of standard models includes an effective band structure and effective short-range magnetic exchange couplings in the spirit of the "t-J" model. In cuprates, the d-wave pairing symmetry is obtained consistently in both types of models [33–37]. In fact, it is well-known that two models of cuprates are intimately linked. These are also reasonable microscopic derivations to support them in capturing essential physics of cuprates [38].

However, for iron-based superconductors, the situation is rather different. The first type of models in iron-based superconductors is generally proposed as [6]

$$\hat{H}_U = \hat{H}_0 + \hat{H}_I, \tag{1}$$

$$\hat{H}_I = \sum_i [\sum_{a\neq b} (J_H \hat{S}_{ai} \cdot \hat{S}_{bi} + U' \hat{n}_{ai\uparrow} \hat{n}_{bi\downarrow}) + U \hat{n}_{ai\uparrow} \hat{n}_{ai\downarrow}], \tag{2}$$

where $\hat{H}_0$ describes the effective multi-orbital band structures based on the five d orbitals of irons [39], a, b label orbitals, and i labels the sites of the iron square lattice. The interaction includes all onsite interactions including the Hund's coupling J_H, intra-orbital repulsive interaction U and inter-orbital repulsive interaction U'. Considering the interaction in the weak to intermediate regions, the model has been treated by a variety of approximate methods including random phase approximation(RPA) [6], perturbative renormalization analysis [40] and numerical functional renormalization analysis (FRG) [41]. The pairing symmetries obtained from the model depend on the detailed structures of Fermi surfaces. In general, the strongest superconductivity is achieved when hole pockets and electron pockets are close to the nesting condition. In this case, the pairing symmetry is the s-wave pairing symmetry, called $s_{\pm}$, which is characterized by the sign change of the superconducting order parameters between the hole and electron pockets in momentum space. With increasing

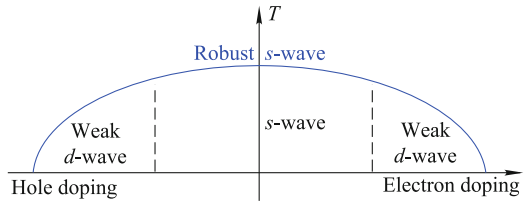

Fig. 2 The sketch of controversial pictures on pairing symmetries of iron-based superconductors as a function of doping: a robust s-wave pairing symmetry vs. theoretical results as indicated by the black text) from the t–U–J_H model in Eq. (2).

hole (or electron) doping, the large anisotropic gap is expected to be developed on hole (or electron) pockets and a transition from the s-wave to d-wave pairing symmetry is expected [42, 43]. In the Fig. 2, we sketch the phase diagram for the pairing symmetries from these theoretical studies. Corresponding to the Fermi surfaces shown in Fig. 1, the results suggest the d-wave pairing for Figs. 1(a), (c), (d) and the s-wave for Fig. 1(b).

A strong message from the above theoretical studies is that there is no universal pairing symmetry in iron-based superconductors. This conclusion is in direct conflict with the experimental observations. Moreover, within these studies, the strongest superconductivity is obtained when hole and electron pockets both exist and are close to the nesting condition. The theory clearly fails to explain the existence of the high-T_c superconductivity at heavily electron doped region of many FeSe-based compounds.

In the second type of models, the starting Hamiltonian [13] is

$$\hat{H}_{tJ} = \hat{\tilde{H}}_0 + \hat{H}_J, \tag{3}$$

$$\hat{H}_J = \sum_{ij} J_{ij} \hat{S}_i \cdot \hat{S}_j, \tag{4}$$

where $\hat{\tilde{H}}_0$ describes the renormalized effective band structure and $\hat{H}_J$ describes the effective magnetic exchange couplings. The pairing symmetry has been studied by including both NN magnetic exchange couplings, $J_{\langle ij\rangle} = J_1$ and next-nearest-neighbor (NNN) ones, $J_{\langle\langle ij\rangle\rangle} = J_2$. Namely, H_J becomes

$$\hat{H}_J = \sum_{\langle ij\rangle} J_1 \hat{S}_i \cdot \hat{S}_j + \sum_{\langle\langle ij\rangle\rangle} J_2 \hat{S}_i \cdot \hat{S}_j. \tag{5}$$

Within this model, a robust s-wave pairing symmetry can be achieved if the NNN AFM exchange coupling J_2 dominates regardless of the presence or absence of the hole pockets [14]. However, if the NN AFM exchange couplings are significant, the pairing symmetry is also expected to deviate from the s-wave [13].

The pairing symmetry in this model is determined easily using the "*correspondence principle*" between Fermi

surface topologies in reciprocal space and the symmetry form factors of short-range magnetic exchange couplings, which was recently specified explicitly by Hu–Ding [44] and Lee–Davis [45]. The principle can be applied to unify the understanding of pairing symmetries in both cuprates and iron-based superconductors. In cuprates, the magnetic exchange coupling is dominated by the NN J_1. If superconductivity stems from the NN J_1 magnetic exchange coupling, we have two choices for pairing symmetries: an extended s-wave and a d-wave. The d-wave form factor associated with J_1 in the superconducting pairing channel is given by $\cos k_x - \cos k_y$, which can open much larger superconducting gaps than the s-wave form factor $\cos k_x + \cos k_y$ on the Fermi surfaces of cuprates. Thus, the d-wave pairing saves more energy than the extended s-wave pairing in the superconducting state. Namely, the d-wave is favored. In iron-based superconductors, if we take J_2 as the source of the superconducting pairing, there are also two choices: an extended s-wave and a d-wave. In the d-wave pairing state, the intra-orbital pairing form factor associated with J_2 is $\sin k_x \sin k_y$, which has much smaller values on Fermi surfaces than the extended s-wave form factor $\cos k_x \cos k_y$. Thus, if J_2 is the dominant magnetic exchange coupling, the strong s-wave superconductivity can be achieved in both Fermi surface topologies shown in Figs. 1(b) and (c). However, it is clear that if J_1 is also important, the d-wave form factor $\cos k_x - \cos k_y$ associated with J_1 can also be very competitive when the electron pockets at the zone corner dominate. In Ref. [14], it is argued that J_1 is inactive in spin-singlet pairing channel in iron-chalcogenides because J_1 based on neutron-scattering experimental data is ferromagnetic (FM), so the s-wave pairing prevails in all iron-chalcogenides [5, 46].

In summary, the first type of model, $\hat{H}_U$, does not support a robust s-wave. In the second type of model, $\hat{H}_{tJ}$, it requires a dominance of J_2 over J_1 to establish a robust s-wave. However, the assumption of the dominance in the second type of model is not well justified for iron-pnictides, where the J_1 value obtained from neutron-scattering experiments can be strongly AFM. Therefore, the robust s-wave symmetry in iron-based superconductors exposes serious limitations and deficiencies in current standard models based on repulsive interaction (or magnetically) driven superconducting mechanisms.

4 Minimum microscopic models used to stabilize s-wave pairing in iron-based superconductors

What are the deficiencies in the standard models for iron-based superconductors and how can they be fixed? In the above section, we showed that the s-wave can be obtained from the J_2 AFM exchange. This provides an important clue. In fact, if we carefully check the electronic structure of iron-based superconductors, it is easy to see that J_1 and J_2 involve different microscopic origins.

First, the difference is already implied in the low-energy effective model that describes the magnetism in iron-based superconductors. Extracted from neutron-scattering experimental data, the value of J_2 is somewhat universal throughout different families of iron-based superconductors [5, 46]. However, this is not the case for J_1. We have shown that the magnetism in iron-based superconductors can be unified by the following effective Hamiltonian,

$$\hat{H}_{JK} = \sum_{\langle ij\rangle}(J_1\hat{S}_i\cdot\hat{S}_j - K(\hat{S}_i\cdot\hat{S}_j)^2) + \sum_{\langle\langle ij\rangle\rangle} J_2\hat{S}_i\cdot\hat{S}_j + \sum_{\langle ij\rangle_{TNN}} J_3\hat{S}_i\cdot\hat{S}_j. \quad (6)$$

This model was proposed as the minimum magnetic model to unify the magnetism in iron-based superconductors [46]. In addition to the J_1 and J_2 terms, the model includes the quadruple spin interaction K term between two NN sites and the third NN (TNN) magnetic exchange coupling J_3 [47]. The K term was first proposed in Ref. [48] to explain the large anisotropy of the effective NN couplings along two different directions in the collinear AFM order state in iron-pnictides.

There are several important observations related to $\hat{H}_{JK}$: (i) the classical phase diagram of the model [46, 49] includes all observed magnetic long-range orders, including both commensurate and incommensurate orders in different families of iron-based superconductors; (ii) J_2 in all iron-based superconductors are universally AFM with a similar value while J_1 is not. In iron-pnictides, J_1 is AFM. However, in iron-chalcogenides, it changes to FM; (iii) the model can even describe the observed magnetic orders in the vacancy ordered states in $K_xFe_{2-y}Se_2$; (iv) J_3 is significant in iron-chalcogenides but small in iron-pnictides; (v) the K term is significant on the NN bonds. The existence of the quadruple term on the NN bonds and the non-universality of the J_1 value suggest that the mechanisms behind J_1 and J_2 are very different.

Second, there is a major difference between the electronic structures of iron-based superconductors and those of cuprates. In cuprates, in the absence of oxygen atoms, the d-orbital of Cu atoms can be treated as localized d-orbital (mottness). The kinetic energy, namely, the effective hopping between two d-orbitals, is caused by the d-p hybridization. This hybridization simultane-

ously generates the magnetic superexchange couplings between two NN Cu sites. Therefore, the magnetism involves a pure superexchange mechanism. If we consider an effective model based on the Cu lattice, the Hubbard term is sufficient to capture the superexchange coupling. Therefore, magnetism and superconducting pairing symmetry can be consistently obtained in both "t-J" and Hubbard models. However, in iron-based superconductors, if we remove the As/Se atoms in the FeAs/Se layer and check the iron lattice, the distance between two NN irons is very short. In fact, the distance is very close to the lattice constant in a 3D body-centered iron metal. Therefore, without As/Se atoms, there is a large hopping between two NN Fe atoms, and the iron lattice itself is a metallic state. The chemical bonding between two NN Fe atoms is not negligible. The difference leads to several important consequences. These include: (i) the hopping through the d-p hybridization, which shows that the superexchange mechanism does not correspond to the hopping defined in the effective Hubbard-type model given in Eq. (2); (ii) the NN hybridization between the d-orbital can also cause magnetism through direct exchange mechanism; (iii) the overlap between two NN d-orbital also suggests that strong repulsive interactions between two NN sites have to be included. Thus, a model with only onsite repulsive interactions is not sufficient to capture the electronic physics of iron-based superconductors. In an effective model with only onsite repulsive interactions given in Eq. (2), J_1 and J_2 are both the leading magnetic coupling terms, and are developed equally. Thus, the different magnetic origins between J_1 and J_2 are not taken into account by Eq. (2).

The above analysis suggests that with only the simple onsite repulsive interaction, $\hat{H}_U$ in Eq. (2) is not sufficient to describe iron-based superconductors. If we consider superconducting pairing driven by repulsive interactions, the onsite repulsive interactions only forbid onsite pairings. Without considering the NN repulsive interactions, the NN pairings generally become the leading contribution to pairing gap functions. In the model given by Eq. (2), as both NN hoppings and NNN hoppings are large, J_1 and J_2 develop equally as the leading magnetic couplings to provide attractive pairing forces. Because of their competition, the pairing symmetry obtained from Eq. (2) is extremely sensitive to changes of the Fermi surfaces.

The above analysis also provides a solution to fix the problem. The existence of chemical bonding between two NN Fe d orbitals suggests that there must be significant repulsive interactions between the NN sites in iron-based superconductors. This repulsive interaction can suppress the attractive interactions generated by the onsite interactions. With both repulsive interactions onsite and between two NN sites, the leading attractive forces must start between the NNN sites so that the robust s-wave can be obtained. Thus, a minimum term that can be added to the Hubbard-type in Eq. (2) is

$$\hat{H}_V = \sum_{\langle ij\rangle,ab} V_{ab}\hat{n}_{ia}\hat{n}_{jb}, \tag{7}$$

where V_{ab} represents the repulsive interactions between two NN sites.

We are not interested in the detailed values of the NN repulsive interaction. In fact, the above term has been considered in many previous studies [50–54]. Here, we can qualitatively argue that this repulsive interaction can serve as an s-wave stabilizer. The effect of this term on pairing can be understood in both real and momentum spaces. In the real space, as repulsive interactions exist both onsite and between NN sites, the attractive force generated for pairing falls to the NNN and the TNN bonds. Namely, the dominated pairing in iron-lattice falls to pairing within each sublattice if we divide the iron lattice into two sublattices: A and B. The inter-sublattice pairing is suppressed. In the reciprocal space, the $\hat{H}_V$ increases the interaction of two Cooper pairs with pairing momentum $(\boldsymbol{k}, -\boldsymbol{k})$ and $(\boldsymbol{k}+\boldsymbol{Q}, -\boldsymbol{k}+\boldsymbol{Q})$ to be attractive. Therefore, the s_{++} pairing can be robust in the presence of only electron pockets at two M points.

To show that $\hat{H}_V$ can serve as a s-wave stabilizer even with a weak coupling approach, we performed an FRG calculation in a parameter region in which an s-wave and d-wave pairing symmetries are very competitive to each other. We take the band parameters provided by Ref. [39]. The unit of all parameters is in the unit of eV. This five-band tight-binding model gives five Fermi surfaces when the chemical potential $\mu = -0.17$. In our calculation, we set the interaction parameters as $U = 4, U' = 4$. The FRG flow demonstrates that s-wave and d-wave instabilities have approximately the same divergence as the decreased momentum cutoff Λ [see Fig. 3(a)]. After adding the NN repulsive interaction V into the interaction part, we obtain a significant enhancement of s-wave instability, which indicates $\hat{H}_V$ tents to induce s-wave pairing symmetry. Figure 3(b) shows the FRG flow when $V_{ab} = V = 1.2$ for any a and b, from it we can see that s-wave is distinctly stronger than d-wave.

It should be noted that we ignored the NNN repulsive interactions between d-orbitals in iron-based superconductors. To justify this, we can compare iron-based superconductors with cuprates, in which the NN d-d repulsive interaction can be ignored. The distance between two NNN Fe atoms is almost identical to the distance between two NN Cu atoms in cuprates. Therefore,

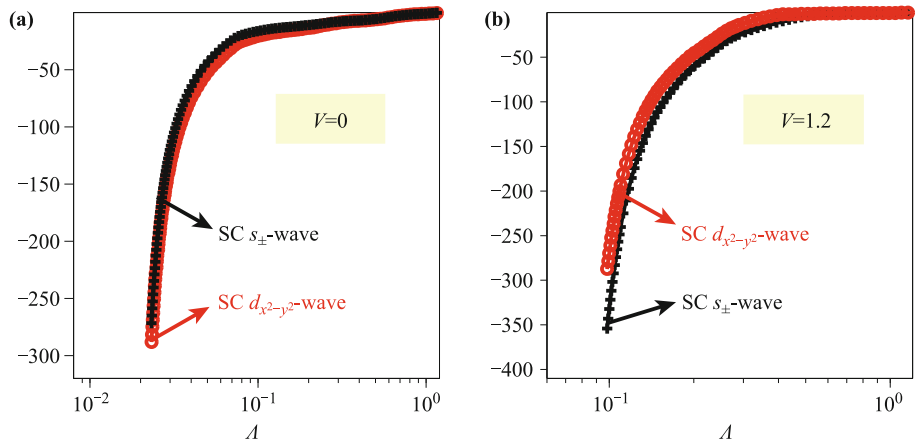

Fig. 3 The FRG flow of superconductivity s-wave and d-wave instabilities for five-band tight-binding model [39] with onsite repulsive interaction U, U' and NN repulsive interaction V in the unit of eV: **(a)** $U = 4, U' = 4, V = 0$, s-wave and d-wave symmetries are very competitive to each other. **(b)** $U = 4, U' = 4, V = 1.2$, the divergence of s-wave is stronger than d-wave after add V.

there is little direct overlap between NNN d-orbitals in iron-based superconductors. Furthermore, with the d-p coupling, as the positive cation atoms are surrounded by the negative anion atoms, the coulomb interactions between NNN d-d orbitals are effectively screened by the surrounding negatively charged anion p-orbitals.

5 Emergence of magnetic selection pairing rule and fundamentals of electronic structures for high-T_c materials

Unconventional high-T_c superconductivity appears to be a rare phenomenon. Only two classes of materials have been discovered accidentally by extensive researches over the past several decades. However, once it occurs, superconductivity is very robust. Their rarity and robustness have already indicated the fundamental difference between unconventional high-T_c superconductors and conventional BCS superconductors, which can almost ubiquitously take place in most metallic systems at low temperature. It is widely believed that the fundamental difference is that the unconventional high-T_c superconductors belong to a new material category called correlated electron systems. Nevertheless, even if the materials are in a different category, explaining the rarity and robustness of high-T_c phenomena is still a fundamental problem as many correlated electron systems have been discovered. Theoretically, we have been accustomed to simplifying correlation physics into an onsite Hubbard interaction for general use. If such a simplified model is applicable to all correlated materials, it is difficult to understand the rarity of high-T_c phenomena.

Combining the rareness dilemma, the robustness of pairing symmetries in both high-T_c superconductors, the above analysis regarding the origin of the robust s-wave pairing symmetry in iron-based superconductors, we can only think of one logistic answer, that is, *high-T_c superconductivity takes place in an electronic environment in which the paired electrons must participate strongly in magnetic superexchange mechanisms. In other words, only magnetic superexchange mechanism drives superconducting pairing.* With this hidden principle, we can understand the rarity problem. Both the d^9 filling configuration in Cu^{2+} in cuprates and the d^6 filling configuration of Fe^{2+} in iron-based superconductors are unique configurations that make the orbital characters on the Fermi surfaces belong to the orbitals with strong involvement in superexchange processes.

Replacing Cu in cuprates or Fe in iron-based superconductors both violate this principle, which explains why the Mn, Co, and Ni-based pnictides are not high-T_c superconductors [55–57]. In cuprates, it is clear that we are required to fill nine electrons to reach $d_{x^2-y^2}$ orbitals. In iron-based superconductors, the three t_{2g} orbitals are orbitals with strong d-p couplings. However, if we carefully consider the local electronic configurations in the Fe-As tetrahedral complex, one of the combinations (or molecular orbitals in the complex) formed by d_{xz} and d_{yz} is strongly coupled to e_g orbitals (primarily $d_{x^2-y^2}$), and was pushed to higher energy. This can be verified by checking the hopping parameters in the five-orbital tight-binding model for iron-based superconductors [6], where it is shown that the largest hopping parameter in the tight-binding model is the NN hopping between $d_{x^2-y^2}$ and d_{yz} along the x axis. The dressed orbital is not a good environment for high-T_c superconductivity. This leaves the other combination of $d_{xz/yz}$ and

d_{xy} as the two pure orbitals that are responsible for our desired high-T_c electronic environment. Thus, the half-filling configuration on these two orbitals requires exactly the total electron filling in the d shells to be around d^6. This is partly the reason why the related Co- and Ni-based compounds are not high-T_c superconductors. In Mn-based compounds, the weights of e_g orbitals are increased dramatically, which is also not good for high-T_c superconductivity. Based on this observation, as e_g orbitals are closely involved with the direct NN exchange mechanism, which is expected to be dominant. In fact, this is indeed the case, as shown in $BaMn_2As_2$, and the direct exchange magnetism is very strong in Mn-based compounds, which leads to a G-type AFM state [58], rather than the E-type AFM state in $BaFe_2As_2$.

The principle also suggests that the effective standardized Hubbard and "t-J" models are only good approximations if all effective hopping parameters in the models stem from the d-p hybridizations. In fact, the presence of a strong correlation effect is generally correlated with the existence of the superexchange processes.

The above magnetic-selection pairing rule, together with the correspondence principle, provides a helpful guide in the search for new unconventional high-T_c superconductors. The first rule specifies the necessary conditions in electronic environments for unconventional high-T_c superconductivity. The second rule provides a direct link between the band structure in the momentum space and the local magnetic physics in real space. It is easy to argue that the rules can be better satisfied in quasi 2D layer materials because of the 2D nature of d-orbitals. For a quasi 2D layer structure constructed by transition metal cation-anion complexes to be a high-T_c candidates the following conditions must be followed:

- *The orbitals (the d-orbitals of cations) responsible for high-T_c superconductivity on Fermi surfaces must be strongly coupled to in-plane anions.* This rule follows the fact that the superexchange is meditated through the anions.The stronger coupling can produce stronger superexchange couplings, thus possible stronger superconductivity. In cuprates, the E_g orbital, $d_{x^2-y^2}$, strongly couples to the p-orbital of in-plane oxygen. In iron-based superconductors, it is the three t_{2g} orbitals that are strongly coupled to the p-orbital of As/Se.
- *The orbitals (the d-orbitals of cations) responsible for high-T_c superconductivity on Fermi surfaces should be relatively higher-energy orbitals in local crystal-field splitting environments.* This rule follows that the orbitals that strongly couple to anions experience a larger crystal-field energy. Therefore, this rule also implies that cation atoms should have high filling in their d-orbital shells in order to achieve possible high-T_c superconductivity. In other words, the second-half transition metal cation atoms, which include both Fe and Cu atoms, are more likely to form potential high-T_c superconductors. Of course, this rule does not completely rule out the possibility of achieving high-T_c superconductivity for the first half transition metal cation atoms.
- *There should be no chemical bonding between anions.* The chemical bonding between anions can generally push the anti-bonding states to higher energy levels, which can strongly suppress the superexchange processes. This is the essential reason why superconductivity and magnetism suddenly disappears in the collapsed $CaFe_2As_2$ phase, where the chemical bonding between two As atoms on neighbor layers are formed [59].
- *The weight of other d-orbital on Fermi surfaces, which do not or only weakly couple to in-plane anions, should be as small as possible.* The combination of the other d-orbitals can strongly suppress superconductivity. It has been commonly known in cuprates that raising the energy level of the d_{z^2} orbital, which increases its presence near Fermi surfaces, strongly suppresses high-T_c superconductivity [60].

In general, the above rules suggest that the electronic environment required to host high-T_c superconductivity must include quasi-2D bands formed dominantly by the d-orbital through d-p couplings near Fermi surfaces.

6 Summary and discussion

In summary, the robustness of s-wave pairing in iron-based superconductors can only be understood by assuming that the pairing is exclusively formed through the superexchange process. More specifically, the superexchange AFM exchange couplings are responsible for superconducting pairing. While this physics is very clear in cuprates, it is not obvious in iron-based superconductors because of the existence of the direct d-d bonding between two NN Fe atoms.

Realizing the origin of pairing from exclusive superexchange AFM significantly affects the search for new high-T_c materials and understanding pairing properties. First, we should aim to design or identify a pure electronic-lattice structure that hosts bands having a dominant contribution from

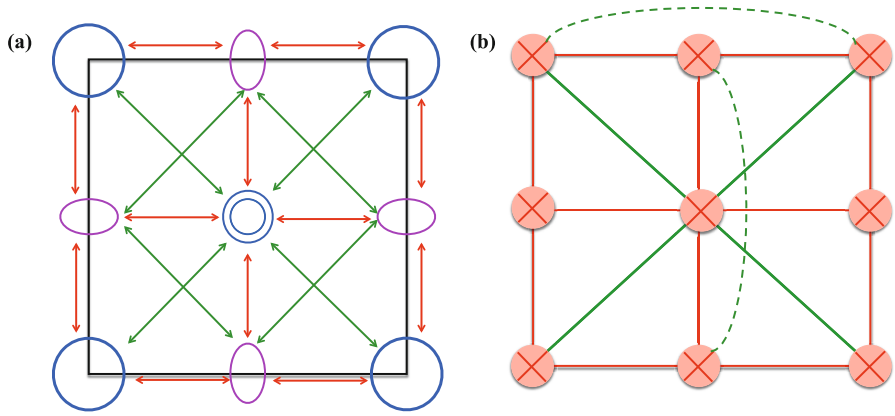

Fig. 4 **(a)** The pairing interactions between different pockets in the 1–Fe unit cell Brillouin zone for iron-based superconductors (the red and green arrows indicate repulsive and attractive pairing interactions, respectively). **(b)** The real space pairing configurations in the Fe lattice for iron-based superconductors (only the two sites linked by the green lines are allowed to be paired).

d-orbitals that involve strong in-plane *d*-*p* hybridization. Second, the superconducting pairing can be better understood in real space compared to in momentum space as the superexchange process is a local process. Figures 4(a) and (b) show a diagram of the leading pairing bonds for iron-based superconductors in real space and its corresponding pairing interaction picture in momentum space. A natural consequence of the real-space picture is that no sign change of the superconducting order parameters on Fermi surfaces is required. This also implies that the earlier argument in the weak-coupling approach regarding the $s_{\pm}$ pairing symmetry, which is based on momentum space, is not entirely correct [61]. Third, it is easy to understand why superconductivity is so robust and in the meanwhile it is so sensitive to the lattice parameter change of the anions as the anions essentially mediates superconducting pairing. For example, the Fe–As–Fe angle is a critical parameter in determining T_c in iron-based superconductors [3]. Finally, the principles also provide an intuitive explanation about why high-T_c superconductivity is absent in many materials with strong magnetic fluctuations.

Contribution J. Yuan carried out the FRG calculations and prepared the Fig. 3. J. P. Hu is responsible for ideas and contexts of the paper. Both authors reviewed the manuscript.

Acknowledgements The work was supported by the National Basic Research Program of China, the National Natural Science Foundation of China (NSFC), and the Strategic Priority Research Program of the Chinese Academy of Sciences.

References

1. Y. Kamihara, T. Watanabe, M. Hirano, and H. Hosono, Iron-based superconductor with $LaO_{1-x}F_xFeAs$ ($x = 0.05-0.12$) with $T_c = 26$ K, *J. Am. Chem. Soc.* 130(11), 3296 (2008)
2. N. Wang, H. Hosono, and P. Dai, Iron-based superconductors: Materials, properties and mechanisms, Pan Stanford Publishing PTE Ltd., 2012
3. D. C. Johnston, The puzzle of high temperature superconductivity in layered iron pnictides and chalcogenides, *Adv. Phys.* 59(6), 803 (2010)
4. E. Dagotto, The unexpected properties of alkali metal iron selenide superconductors, *Rev. Mod. Phys.* 85(2), 849 (2013)
5. P. C. Dai, J. P. Hu, and E. Dagotto, Magnetism and its microscopic origin in iron-based high-temperature superconductors, *Nat. Phys.* 8(10), 709 (2012)
6. P. J. Hirschfeld, M. M. Korshunov, and I. I. Mazin, Gap symmetry and structure of Fe-based superconductors, *Rep. Prog. Phys.* 74(12), 124508 (2011)
7. J. P. Hu, Iron-based superconductors as odd parity superconductors, *Phys. Rev. X* 3(3), 031004 (2013)
8. N. N. Hao and J. P. Hu, Odd parity pairing and nodeless antiphase *s* in iron-based superconductors, *Phys. Rev. B* 89(4), 045144 (2014)
9. C. C. Tsuei and J. R. Kirtley, Pairing symmetry in cuprate superconductors, *Rev. Mod. Phys.* 72(4), 969 (2000)
10. D. J. Scalapino, The cuprate pairing mechanism, *Science* 284(5418), 1282 (1999)
11. P. W. Anderson, P. A. Lee, M. Randeria, T. M. Rice, N. Trivedi, and F. C. Zhang, The physics behind high-temperature superconducting cuprates: The "plain vanilla" version of RVB, *J. Phys.: Condens. Matter* 16(24), R755 (2004)
12. Q. M. Si and E. Abrahams, Strong correlations and magnetic frustration in the high-T_c iron pnictides, *Phys. Rev. Lett.* 101(7), 076401 (2008)
13. K. J. Seo, B. A. Bernevig, and J. P. Hu, Pairing symmetry in a two-orbital exchange coupling model of oxypnictides, *Phys. Rev. Lett.* 101(20), 206404 (2008)

14. C. Fang, Y. L. Wu, R. Thomale, B. A. Bernevig, and J. Hu, Robustness of *s*-wave pairing in electron-overdoped $A_{1-y}Fe_{2-x}Se_2$, *Phys. Rev. X* 1(1), 011009 (2011)
15. P. Richard, T. Qian, and H. Ding, ARPES measurements of the superconducting gap of Fe-based superconductors and their implications to the pairing mechanism, arXiv: 1503.07269 (2015)
16. Q. Fan, W. H. Zhang, X. Liu, Y. J. Yan, M. Q. Ren, R. Peng, H. C. Xu, B. P. Xie, J. P. Hu, T. Zhang, and D. L. Feng, Plain *s*-wave superconductivity in single-layer FeSe on $SrTiO_3$ probed by scanning tunneling microscopy, arXiv: 1504.02185 (2015)
17. X. H. Niu, R. Peng, H. C. Xu, Y. J. Yan, J. Jiang, D. F. Xu, T. L. Yu, Q. Song, Z. C. Huang, Y. X. Wang, B. P. Xie, X. F. Lu, N. Z. Wang, X. H. Chen, Z. Sun, and D. L. Feng, Surface electronic structure and isotropic superconducting gap in $Li_{0.8}Fe_{0.2}$OHFeSe, arXiv: 1506.02825 (2015)
18. L. Zhao, A. Liang, D. Yuan, Y. Hu, D. Liu, J. Huang, S. He, B. Shen, Y. Xu, X. Liu, L. Yu, G. Liu, H. Zhou, Yulong Huang, X. Dong, F. Zhou, Z. Zhao, C. Chen, Z. Xu, and X. J. Zhou, Common electronic origin of superconductivity in (Li,Fe)OHFeSe bulk superconductor and single-layer FeSe/$SrTiO_3$ films, arXiv: 1505.6361 (2015)
19. P. A. Lee and X. G. Wen, Spin-triplet *p*-wave pairing in a three-orbital model for iron pnictide superconductors, *Phys. Rev. B* 78(14), 144517 (2008)
20. V. Cvetkovic and O. Vafek, Space group symmetry, spin-orbit coupling, and the low-energy effective hamiltonian for iron-based superconductors, *Phys. Rev. B* 88(13), 134510 (2013)
21. Y. Zhang, L. X. Yang, M. Xu, Z. R. Ye, F. Chen, C. He, H. C. Xu, J. Jiang, B. P. Xie, J. J. Ying, X. F. Wang, X. H. Chen, J. P. Hu, M. Matsunami, S. Kimura, and D. L. Feng, Nodeless superconducting gap in $A_xFe_2Se_2$ (A=K,Cs) revealed by angle-resolved photoemission spectroscopy, *Nat. Mater.* 10(4), 273 (2011)
22. Q. Y. Wang, Z. Li, W. H. Zhang, Z. C. Zhang, J. S. Zhang, W. Li, H. Ding, Y. B. Ou, P. Deng, K. Chang, J. Wen, C. L. Song, K. He, J. F. Jia, S. H. Ji, Y. Y. Wang, L. L. Wang, X. Chen, X. C. Ma, and Q. K. Xue, Interface-induced high-temperature superconductivity in single unit-cell FeSe films on $SrTiO_3$, *Chin. Phys. Lett.* 29(3), 037402 (2012)
23. S. L. He, J. He, W. Zhang, L. Zhao, D. Liu, X. Liu, D. Mou, Y. B. Ou, Q. Y. Wang, Z. Li, L. Wang, Y. Peng, Y. Liu, C. Chen, L. Yu, G. Liu, X. Dong, J. Zhang, C. Chen, Z. Xu, X. Chen, X. Ma, Q. Xue, and X. J. Zhou, Phase diagram and electronic indication of high-temperature superconductivity at 65 K in single-layer FeSe films, *Nat. Mater.* 12(7), 605 (2013)
24. S. Y. Tan, Y. Zhang, M. Xia, Z. Ye, F. Chen, X. Xie, R. Peng, D. Xu, Q. Fan, H. Xu, J. Jiang, T. Zhang, X. Lai, T. Xiang, J. Hu, B. Xie, and D. Feng, Interface-induced superconductivity and strain-dependent spin density waves in FeSe/$SrTiO_3$ thin films, *Nat. Mater.* 12(7), 634 (2013)
25. M. Xu, Q. Q. Ge, R. Peng, Z. R. Ye, J. Jiang, F. Chen, X. P. Shen, B. P. Xie, Y. Zhang, A. F. Wang, X. F. Wang, X. H. Chen, and D. L. Feng, Evidence for an *s*-wave superconducting gap in $K_xFe_{2-y}Se_2$ from angle-resolved photoemission, *Phys. Rev. B* 85(22), 220504 (2012)
26. X. Liu, L. Zhao, S. He, J. He, D. Liu, D. Mou, B. Shen, Y. Hu, J. Huang, and X. J. Zhou, Electronic structure and superconductivity of FeSe-related superconductors, *J. Phys.: Condens. Matter* 27(18), 183201 (2015)
27. I. I. Mazin, Symmetry analysis of possible superconducting states in $K_xFe_2Se_2$ superconductors, *Phys. Rev. B* 84(2), 024529 (2011)
28. F. F. Tafti, A. Ouellet, A. Juneau-Fecteau, S. Faucher, M. Lapointe-Major, N. Doiron-Leyraud, A. F. Wang, X.G. Luo, X. H. Chen, and L. Taillefer, Universal V-shaped temperature-pressure phase diagram in the iron-based superconductors KFe_2As_2, $RbFe_2As_2$, and $CsFe_2As_2$, *Phys. Rev. B* 91(5), 054511 (2015)
29. Y. Ota, K. Okazaki, Y. Kotani, T. Shimojima, W. Malaeb, S. Watanabe, C.T. Chen, K. Kihou, C. H. Lee, A. Iyo, H. Eisaki, T. Saito, H. Fukazawa, Y. Kohori, and S. Shin, Evidence for excluding the possibility of *d*-wave superconducting-gap symmetry in Ba-doped KFe_2As_2, *Phys. Rev. B* 89(8), 081103 (2014)
30. K. Okazaki, Y. Ota, Y. Kotani, W. Malaeb, Y. Ishida, T. Shimojima, T. Kiss, S. Watanabe, C.T. Chen, K. Kihou, C. H. Lee, A. Iyo, H. Eisaki, T. Saito, H. Fukazawa, Y. Kohori, K. Hashimoto, T. Shibauchi, Y. Matsuda, H. Ikeda, H. Miyahara, R. Arita, A. Chainani, and S. Shin, Octet-line node structure of superconducting order parameter in KFe_2As_2, *Science* 337(6100), 1314 (2012)
31. Y. Zhang, Z. R. Ye, Q. Q. Ge, F. Chen, J. Jiang, M. Xu, B. P. Xie, and D. L. Feng, Nodal superconducting-gap structure in ferropnictide superconductor $BaFe_2(As_{0.7}P_{0.3})_2$, *Nat. Phys.* 8(5), 371 (2012)
32. X. Qiu, S. Y. Zhou, H. Zhang, B. Y. Pan, X. C. Hong, Y. F. Dai, M. J. Eom, J. S. Kim, Z. R. Ye, Y. Zhang, D. L. Feng, and S. Y. Li, Robust nodal superconductivity induced by isovalent doping in $Ba(Fe_{1-x}Ru_x)_2As_2$ and $BaFe_2(As_{1-x}P_x)_2$, *Phys. Rev. X* 2(1), 011010 (2012)
33. N. Bickers, D. J. Scalapino, and R. T. Scalettar, Cdw and sdw mediated pairing interactions, *Int. J. Mod. Phys. B* 01(03n04), 687 (1987)
34. M. Inui, S. Doniach, P. Hirschfeld, and A. Ruckenstein, Coexistence of antiferromagnetism and superconductivity in a mean-field theory of high-T_c superconductors, *Phys. Rev. B* 37(4), 2320 (1988)
35. C. Gros, D. Poilblanc, T. M. Rice, and F. C. Zhang, Superconductivity in correlated wavefunctions, *Physica C* 153–155, 543 (1988)
36. G. Kotliar and J. Liu, Superexchange mechanism and *d*-wave superconductivity, *Phys. Rev. B* 38(7), 5142 (1988)
37. W. Metzner, M. Salmhofer, C. Honerkamp, V. Meden, and K. Schnhammer, Functional renormalization group approach

to correlated fermion systems, *Rev. Mod. Phys.* 84(1), 299 (2012)

38. F. C. Zhang and T. M. Rice, Effective hamiltonian for the superconducting Cu oxides, *Phys. Rev. B* 37(7), 3759 (1988)
39. S. Graser, T. A. Maier, P. J. Hirschfeld, and D. J. Scalapino, Near-degeneracy of several pairing channels in multiorbital models for the Fe pnictides, *New J. Phys.* 11(2), 025016 (2009)
40. S. Maiti, M. M. Korshunov, T. A. Maier, P. J. Hirschfeld, and A. V. Chubukov, Evolution of the superconducting state of Fe-based compounds with doping, *Phys. Rev. Lett.* 107(14), 147002 (2011)
41. F. Wang, H. Zhai, and D. H. Lee, Nodes in the gap function of LaFePo, the gap function of the Fe(Se,Te) systems, and the STM signature of the s pairing, *Phys. Rev. B* 81(18), 184512 (2010)
42. T. A. Maier, S. Graser, P. J. Hirschfeld, and D. J. Scalapino, *d*-wave pairing from spin fluctuations in the $K_xFe_{2-y}Se_2$ superconductors, *Phys. Rev. B* 83(10), 100515 (2011)
43. R. Thomale, C. Platt, W. Hanke, J. Hu, and B. A. Bernevig, Exotic *d*-wave superconductivity in strongly hole doped $K_xBa_{1-x}Fe_2As_2$, *Phys. Rev. Lett.* 107(11), 117001 (2011)
44. J. P. Hu and H. Ding, Local antiferromagnetic exchange and collaborative Fermi surface as key ingredients of high temperature superconductors, *Sci. Rep.* 2, 381 (2012)
45. J. S. Davis and D. H. Lee, Concepts relating magnetic interactions, interwined electronic orders, and strongly correlated superconductivity, *Proc. Natl. Acad. Sci. USA* 110(44), 17623 (2013)
46. J. P. Hu, B. Xu, W. Liu, N. N. Hao, and Y. Wang, Unified minimum effective model of magnetic properties of iron-based superconductors, *Phys. Rev. B* 85(14), 144403 (2012)
47. F. Ma, W. Ji, J. Hu, Z. Y. Lu, and T. Xiang, First-principles calculations of the electronic structure of tetragonal alpha-FeTe and alpha-FeSe crystals: Evidence for a bicollinear antiferromagnetic order, *Phys. Rev. Lett.* 102, 177003 (2009)
48. A. L. Wysocki, K. D. Belashchenko, and V. P. Antropov, Consistent model of magnetism in ferropnictides, *Nat. Phys.* 7(6), 485 (2011)
49. J. K. Glasbrenner, I. I. Mazin, H. Jeschke, P. J. Hirschfeld, and R. Valent, Effect of magnetic frustration on nematicity and superconductivity in Fe chalcogenides, arXiv: 1501.04946 (2015)
50. T. Miyake, T. Kosugi, S. Ishibashi, and K. Terakura, Electronic structure of novel superconductor $Ca_4Al_2O_6Fe_2As_2$, *J. Phys. Soc. Japan* 79(12), 123713 (2010)
51. O. Andersen and L. Boeri, On the multi-orbital band structure and itinerant magnetism of iron-based superconductors, *Annalen der Physik,* 1, 8 (2011)
52. Z. P. Yin, K. Haule, and G. Kotliar, Kinetic frustration and the nature of the magnetic and paramagnetic states in iron pnictides and iron chalcogenides, *Nat. Mater.* 10(12), 932 (2011)
53. K. Suzuki, H. Usui, S. Iimura, Y. Sato, S. Matsuishi, H. Hosono, and K. Kuroki, Model of the electronic structure of electron-doped iron-based superconductors: Evidence for enhanced spin fluctuations by diagonal electron hopping, *Phys. Rev. Lett.* 113(2), 027002 (2014)
54. D. Guterding, H. O. Jeschke, P. J. Hirschfeld, and R. Valenti, Unified picture of the doping dependence of superconducting transition temperatures in alkali metal/ammonia intercalated FeSe, *Phys. Rev. B* 91, 041112(R) (2015)
55. F. Ronning, N. Kurita, E. D. Bauer, B. L. Scott, T. Park, T. Klimczuk, R. Movshovich, and J. D. Thompson, The first order phase transition and superconductivity in $BaNi_2As_2$ single crystals, *J. Phys.: Condens. Matter* 20(34), 342203 (2008)
56. A. S. Sefat, D. J. Singh, R. Jin, M. A. McGuire, B. C. Sales, and D. Mandrus, Renormalized behavior and proximity of $BaCo_2As_2$ to a magnetic quantum critical point, *Phys. Rev. B* 79(2), 024512 (2009)
57. Y. Singh, A. Ellern, and D. C. Johnston, Magnetic, transport, and thermal properties of single crystals of the layered arsenide $BaMn_2As_2$, *Phys. Rev. B* 79(9), 094519 (2009)
58. D. Gu, X. Dai, C. Le, L. Sun, Q. Wu, B. Saparov, J. Guo, P. Gao, S. Zhang, Y. Zhou, C. Zhang, S. Jin, L. Xiong, R. Li, Y. Li, X. Li, J. Liu, A. S. Sefat, J. Hu, and Z. Zhao, Robust antiferromagnetism preventing superconductivity in pressurized $(Ba_{0.61}K_{0.39})Mn_2Bi_2$, *Sci. Rep.* 4, 7342 (2014)
59. R. Yang, C. Le, L. Zhang, B. Xu, W. Zhang, K. Nadeem, H. Xiao, J. Hu, and X. Qiu, Formation of As-As bond and its effect on absence of superconductivity in collapsed tetragonal phase of $Ca_{0.86}Pr_{0.14}Fe_2As_2$: An optical spectroscopy study, *Phys. Rev. B* 91(22), 224507 (2015)
60. H. Sakakibara, K. Suzuki, H. Usui, K. Kuroki, R. Arita, D. J. Scalapino, and H. Aoki, Three-orbital study on the orbital distillation effect in the high-T_c cuprates, *Phys. Proc.* 45, 13 (2013)
61. I. Mazin, D. J. Singh, M. D. Johannes, and M. H. Du, Unconventional superconductivity with a sign reversal in the order parameter of $LaFeAsO_{1-x}F_x$, *Phys. Rev. Lett.* 101(5), 057003 (2008)